

# Immediate and Time-Dependent Compression of Tire Derived Aggregate

Joseph Wartman, M.ASCE<sup>1</sup>; Mark F. Natale<sup>2</sup>; and Patrick M. Strenk, M.ASCE<sup>3</sup>

**Abstract:** This paper examines immediate and time-dependent compression of tire derived aggregate (TDA) and TDA-soil composites. To accommodate large particle sizes, modified experimental devices were developed and used to test tire chips and tire shreds. Immediate compression of TDA, which results almost entirely from the reduction of pore volume, increases with TDA content and tire particle size. The secant constrained modulus ( $M_{sec}$ ) of TDA defined over the stress range of 0–50 kPa varied from a low of 255 kPa (100% tire shreds) to a high of 1,320 kPa (50% tire chips). A characteristic relationship between strain and time exists for TDA and TDA composites under one-dimensional confined compression. Time-dependent deformation is well described by the modified secondary compression index ( $C_{\alpha\epsilon}$ ), which ranged from 0.0010 (50% tire chips) to 0.0074 (100% tire chips). Time-dependent deformation was inversely proportional to sand content, with the most significant changes resulting from the addition of 15% sand. Both applied stress and tire particle size appear to have a negligible effect on time-dependent compression of TDA. Based on the findings of this study it is recommended that practitioners assess time-dependent settlement when designing a TDA structure and if necessary incorporate design features to accommodate these settlements.

**DOI:** 10.1061/(ASCE)1090-0241(2007)133:3(245)

**CE Database subject headings:** Tires; Recycling; Triaxial test; Compressibility; Creep; Settlement; Deformation.

## Introduction

Owing to its light weight, favorable drainage characteristics, and widespread availability, *tire derived aggregate* (Humphrey 2004a) is one of the most popular recycled materials used in geotechnical applications such as embankment and retaining wall construction. Tire derived aggregate, or TDA, is an engineered material made by reducing scrap tires into particle sizes ranging from 25 to 305 mm (Humphrey 2004b). Finely graded TDA (12–50 mm) is typically referred to as *tire chips* whereas TDA having larger particle sizes (50–305 mm) is classified as *tire shreds* [ASTM D6270 (ASTM 1998b)]. In some applications, tire chips or shreds are mixed with soil to create TDA-soil composites. As particulate media, TDA has strength characteristics that are in many respects similar to those of conventional soils and aggregates; however, because of its low elastic modulus, TDA is unique in that it exhibits a very high degree of compressibility.

The shear strength of TDA and TDA composites has been the subject of previous laboratory investigations (e.g., Humphrey et al. 1993; Cosgrove 1995; Foose et al. 1996; Wu et al. 1997; Moo-Young et al. 2003) and is well understood today. Yet, as noted by Bosscher et al. (1997), it is *deformation* rather than the strength characteristics of TDA that ultimately govern its design and performance in most applications. Accordingly, studies have evaluated the compressibility characteristics of TDA and TDA composites (e.g., Humphrey and Manion 1992; Ahmed 1993; Edil and Bosscher 1994; Tatlisoz et al. 1997). Most of these studies have focused on evaluating immediate compressibility; however, case histories have clearly shown that when used in geotechnical applications TDA and TDA composites continue to deform over time periods that extend well beyond the initial application of load (e.g., Bosscher et al. 1993; Tweedie et al. 1998; Humphrey et al. 2000; Dickson et al. 2001; Hoppe and Mullen 2004; Salgado et al. 2003; Zornberg et al. 2004b). These time-dependent deformations occur at a generally constant rate over logarithmic cycles of time and can approach strains of 5% or more after 1 to 2 years (Fig. 1 and Table 1). This has led some to question if TDA and TDA composites are appropriate for projects whose long-term performance and serviceability will be affected by deformation.

This study investigates the mechanisms that control and the factors that affect immediate and time-dependent compression of TDA and TDA composites. Modified experimental devices were developed to accommodate the large particle sizes of the tire chips and tire shreds used in this study. It is shown that TDA exhibits a high degree of both immediate and time-dependent compression. The magnitude of immediate compression in TDA and TDA composites is principally a function of tire particle size, TDA content, and applied stress, while time-dependent compression is largely a function of TDA content and time.

<sup>1</sup>Associate Professor, Dept. of Civil, Architectural and Environmental Engineering, Drexel Univ., 3141 Chestnut St., Philadelphia, PA 19104.

<sup>2</sup>Graduate Student Researcher, Dept. of Civil, Architectural and Environmental Engineering, Drexel Univ., 3141 Chestnut St., Philadelphia, PA 19104.

<sup>3</sup>Graduate Student Researcher, Dept. of Civil, Architectural and Environmental Engineering, Drexel Univ., 3141 Chestnut St., Philadelphia, PA 19104.

Note. Discussion open until August 1, 2007. Separate discussions must be submitted for individual papers. To extend the closing date by one month, a written request must be filed with the ASCE Managing Editor. The manuscript for this paper was submitted for review and possible publication on June 16, 2005; approved on June 7, 2006. This paper is part of the *Journal of Geotechnical and Geoenvironmental Engineering*, Vol. 133, No. 3, March 1, 2007. ©ASCE, ISSN 1090-0241/2007/3-245–256/\$25.00.

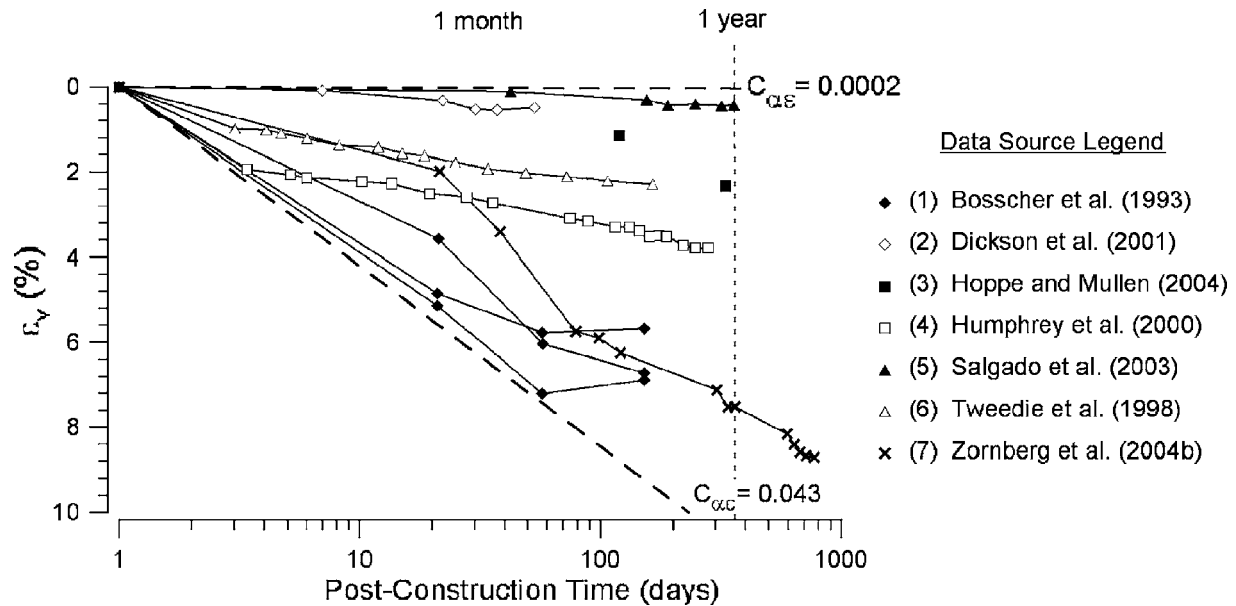


**Fig. 1.** Summary of case studies of long-term deformation under constant load for TDA and TDA composite structures. Dashed lines show the approximate bounds of the data and associated secondary compression indices ( $C_{\alpha\varepsilon}$ ) [the data for Dickson et al. (2001) and Salgado et al. (2003) represent the average of multiple instrumentation points].

### Previous Experimental Investigations

Previous experimental studies have characterized the physical properties of TDA. One of the most beneficial characteristics of TDA is its low weight, which makes it an ideal material for use over low strength, compressible soils. The light weight of TDA is due to its low specific gravity ( $G_s$ ), which typically ranges from 1.05 to 1.36 [depending on metal content from steel reinforcing belts; Humphrey and Manion (1992); Edil and Bosscher (1994)] and this ultimately translates into compacted unit weight ( $\gamma$ ) values that are on the order of 5.8–6.2 kN/m<sup>3</sup>, or about a third of that of conventional soils. The unit weight of TDA composites increases in proportion to soil content, thus adversely affecting one of TDA’s most favorable characteristics.

Investigators have considered the shear strength characteristics of TDA both when used alone and when added in small amounts to “reinforce” proportionally larger quantities of soil (e.g., Foose et al. 1996; Zornberg et al. 2004a). Owing to the difficulty of

testing materials with large particles, many of these experimental studies have considered tire chips rather than tire shreds. Nevertheless, recent work has found that the shear strength of TDA is generally scale-independent (Yang et al. 2002; Strenk et al. 2007), thus implying that the results of laboratory tests on tire chips are representative of larger sized tire shreds. In practice, the friction angle of TDA is commonly taken to be 25° (Strenk et al. 2007). Edil (2002) noted that because TDA has a lower elastic modulus than soil, relatively large strains are required to mobilize ultimate shear resistance. In composite applications, Foose et al. (1996) found that when included at volumetric contents of up to 30%, TDA serves to reinforce and thereby enhance the strength of soil. When the tire content exceeds 30–40%, TDA composites essentially begin to behave as a TDA mass with sand occupying the pore space. The shear strength of these higher TDA content materials is often comparable to that of TDA alone.

Immediate compression is an important property of TDA that can affect the design and performance of pavement systems and

**Table 1.** Characteristics of Case Studies for TDA and TDA Composite Structures

No.	Reference	Structure type	$D_{max}$ (cm)	$\gamma$ (kN/m <sup>3</sup> ) <sup>a</sup>	Composition (tires/soil) <sup>b</sup>	TDA layer thickness (m) <sup>c</sup>	Nature of loading
1	Bosscher et al. (1993)	Roadway embankment	i) 4.0, 7.5 ii) 7.5	i) 5.0, 5.5 ii) 11.8	i) 100/0 ii) 50/50	1.5	Traffic
2	Dickson et al. (2001)	Roadway embankment	30.5	6.0	100/0	3.0	Surcharge
3	Hoppe and Mullen (2004)	Roadway embankment	25.0	—	50/50	4.5	Surcharge
4	Humphrey et al. (2000)	Bridge abutment approach	30.5	8.8	100/0	4.3	Surcharge, traffic
5	Salgado et al. (2003)	Roadway embankment	3.8	11.5	50/50	2.1	Traffic
6	Tweedie et al. (1998)	Retaining wall	7.5	6.9	100/0	4.8	Surcharge
7	Zornberg et al. (2004b)	Roadway embankment	15.0	—	20/80 <sup>d</sup>	1.2	Traffic

<sup>a</sup>Corresponding to in-place, compressed unit weight (lift thicknesses ranging from 20.3 to 30.5 cm).

<sup>b</sup>Reported TDA compositions are percentages by volume.

<sup>c</sup>Soil cap thickness over the TDA layer ranges from 0.3 to 1.9 m, with the exception of Tweedie et al. (1998).

<sup>d</sup>The weight composition reported by Zornberg et al. (2004b) was converted to volume composition based on an assumed unit weight.

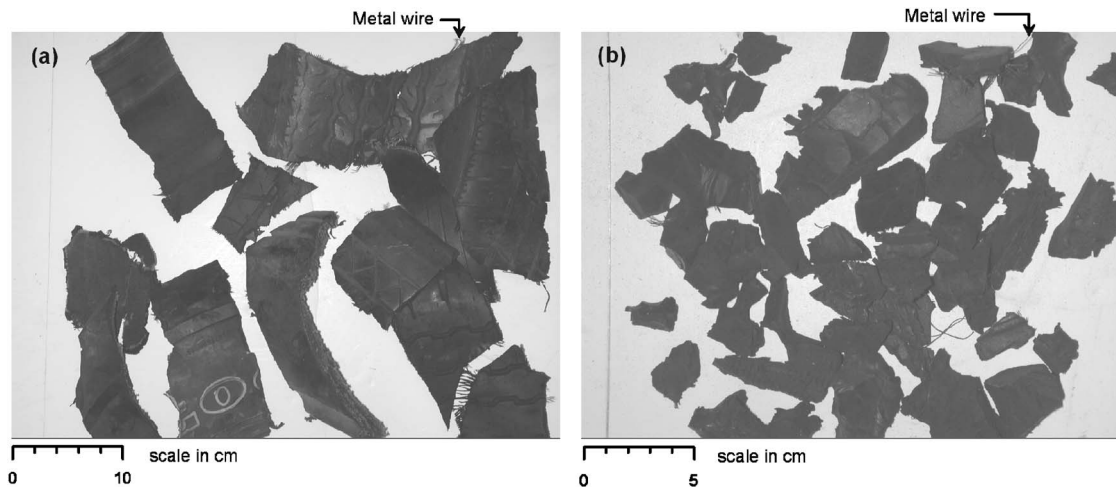


**Fig. 2.** Photograph of the tire shreds (a) and tire chips (b) used in this study

other project components subjected to transient loads such as traffic. Accordingly, researchers including Humphrey and Manion (1992), Edil and Bosscher (1994), and Tatlisoz et al. (1997) have investigated the one-dimensional compression characteristics of TDA and TDA composites. Because of difficulties adapting conventional laboratory test equipment to large size tire shreds, nearly all of the previous studies have focused on tire chips. In contrast to shear strength, Strenk et al. (2007) found that constrained modulus, and by association, compressibility, exhibits a moderate degree of scale dependence, with large TDA particles yielding higher levels of compression. Therefore caution is warranted when extrapolating the results of immediate compression tests from tire chips to tire shreds. Humphrey and Manion (1992) found that TDA exhibits a high degree of compressibility upon initial loading, especially at low stresses (0–70 kPa). As the applied stress was increased, TDA became progressively less compressible. This nonlinear compression response can be represented with a hyperbolic compression model (Tatlisoz et al. 1997). It has been suggested that because of its low elastic modulus, the mechanisms that govern immediate compression of TDA differ from those of conventional soils, whose solid phase is relatively incompressible (e.g., Yang et al. 2002). Bosscher et al. (1997) and Youwai and Bergado (2003) have theorized that immediate compression in TDA occurs from two distinct mechanisms: Reduction of pore volume and deformation of the tire particles. Youwai and Bergado (2003) indicated that for this reason the traditional notion of void ratio may not be relevant to TDA.

Tatlisoz et al. (1997) found that compressibility of TDA (tire chips) composites is inversely proportional to soil content, with the most significant reductions in compressibility occurring for mixtures having soil contents up to 30%. Tatlisoz et al. (1997) also compared the time-dependent compression of TDA to that of TDA-silt and TDA-sand composites (30% TDA) and found that the addition of soil reduced the long-term compression of TDA. Long-term compression tests on TDA were also performed by Humphrey et al. (1992), who measured time-dependent vertical strains of about 1% over 30 days.

### Laboratory Experimental Program

The experimental program was designed to study the mechanisms of immediate and time-dependent compression of TDA and TDA

composites and to determine how compression response varies with soil content and tire particle size. Tire derived aggregate was the primary component of the composites, reflecting an interest in maximizing reuse of tires and maintaining a low unit weight, rather than reinforcing larger quantities of soil. The testing program considered TDA and TDA-sand composites containing 100, 85, 65, and 50% TDA by volume. Experiments were also performed on sand specimens (0% TDA) so that the compressibility of TDA could be compared to that of a conventional soil.

One-dimensional compression experiments were performed under stresses up to 200 kPa. Although TDA has been placed to heights in excess of 10 m in a limited number of cases, a range of 2 to 3 m (corresponding to vertical stresses of 16–25 kPa) is more common today as a measure to minimize the risk of internal heating reactions [Humphrey 2004b; ASTM D6270 (ASTM 1998b)]. Experiments were performed under both one-dimensional confined compression and isotropic compression. The latter tests were performed on tire chip TDA specimens in a triaxial cell under fully saturated conditions so that changes in specimen volume and pore volume could be simultaneously measured, thereby allowing the mechanisms governing immediate compression in TDA to be identified. The one-dimensional compression tests were performed on air-dried tire chip and tire shred specimens. Although TDA can become wet in field applications, research has shown that water has an insignificant affect on its compression characteristics (Tatlisoz et al. 1997).

### Materials

The tire chips and tire shreds used in the study were produced at a tire recycling facility located in southeastern Pennsylvania. The recycling facility accepts automobile and small truck tires, which are subsequently processed into a range of commercial products including TDA. The tires were processed by first removing the inner portion of the sidewalls and then placing the remaining material in a shredder, where it was cut into rectangular-shaped tire shreds. Fig. 2(a) is a photograph of the processed tire shreds. The shreds are primarily comprised of synthetic rubber compounds with a minor amount of residual metal wire from the steel belts. The large size of the tire shreds precludes particle size characterization by conventional sieve analysis and therefore an alternative approach was used to characterize the size and shape of the shreds. Fifty pieces were randomly selected from a repre-

**Table 2.** Average Measured Dimensions of the Tire Shreds<sup>a</sup>

Statistical property	Tire shred dimensions		
	Thickness (cm)	Width (cm)	Length (cm)
Average ( $\bar{x}$ )	1.14	7.53	17.84
Standard deviation ( $\sigma$ )	0.28	1.68	6.78

<sup>a</sup>For a sample size ( $n$ ) of 50.

sentative lot of tire shreds and measured to determine their average length, width, and thickness. The results, which are summarized in Table 2, indicate that the shreds had an average maximum particle dimension ( $D_{max}$ ) of 17.8 cm and aspect ratio of approximately 2.4. A specific gravity of 1.31 was determined for the tire shreds using conventional test methods [ASTM C127 (ASTM 2005)].

The tire chips were processed in the same manner as tire shreds and subsequently passed through a secondary shredder to further reduce their particle size [Fig. 2(b)]. To minimize metal content, the tire chips were passed through a magnetic field, leaving a product that contained less than 5% metal (by weight). The particle size distribution of the tire chips was assessed using conventional sieve analyses. The results presented in Fig. 3 show that the tire chips classified as poorly graded gravel (GP) based on the Unified Soil Classification System [USCS; ASTM D2487 (ASTM 1998a)] with a maximum particle size ( $D_{max}$ ) of 3 cm. Reflecting their lower metal content, the specific gravity of the tire chips was 1.07, or about 80% that of tire shreds.

The TDA composites were mixed with a uniformly graded, medium subangular sand classified as SP based on USCS. The sand, whose grain size distribution is included in Fig. 3, was selected to be representative of a conventional granular fill soil. The sand had a maximum dry density ( $\gamma$ ) of 16.04 kN/m<sup>3</sup> based on the Modified Proctor compaction test [ASTM D1557 (ASTM 2000a)]. Table 3 summarizes the physical properties of all materials used in the study.

### Specimen Preparation

The TDA composites were produced by combining TDA with sand and thoroughly mixing the materials using hand tools until

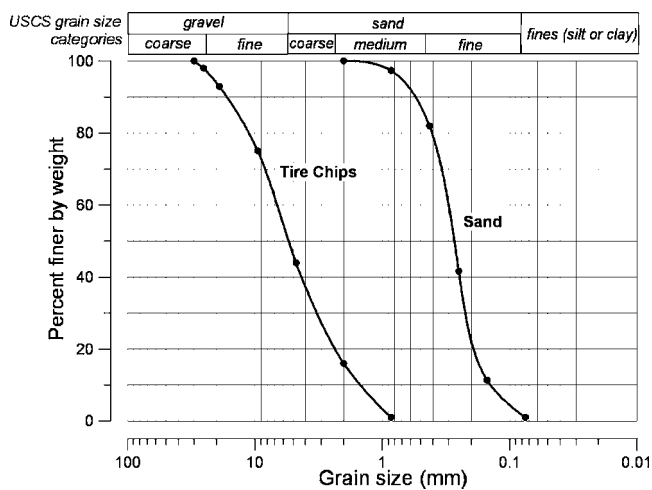


**Fig. 3.** Particle size distributions for tire chips and sand used in this study

**Table 3.** Physical Properties of the Materials Used in This Study

Material	$\gamma$ (kN/m <sup>3</sup> )	$n^b$	$e^b$	$G_s$	$D_{max}$ (cm)
Tire chips	6.46 <sup>a</sup>	0.38	0.62	1.07	3.0
Tire shreds	4.74 <sup>a</sup>	0.63	1.71	1.31	— <sup>c</sup>
Sand	16.04	0.37	0.58	2.59	0.2

<sup>a</sup>Based on a selected compaction energy of 600 kN m/m<sup>3</sup>.

<sup>b</sup>As-compacted porosity and void ratio values.

<sup>c</sup>Refer to Table 2 for tire shred particle size.

they appeared consistent. Early mixing trials using dry sand proved unsuccessful due to material segregation; however, adding a minor amount of water to the mixture (water content  $\approx 2\%$ ) provided enough capillarity to keep the materials from separating. This modified preparation procedure consistently produced uniformly mixed specimens.

Commensurate with traditional TDA construction practice, the specimens were compacted prior to testing. Recognizing that field quality control assessment procedures for TDA are usually based on a compactive energy criterion (i.e., specified number of equipment passes) rather than traditional dry density requirements, special laboratory compaction procedures were adopted to ensure uniformity among the test specimens. The relationship between compaction energy and TDA density was determined by performing compaction experiments using a 15.2 by 15.2 cm, 5.14 kg drop hammer. In separate trials, tire chips and shreds were placed in a 305 mm square by 305 mm high specimen container (a detailed description follows in the next section) in five layers (pre-compaction lift thicknesses of 2.4 cm) and compacted until changes in dry density became insignificant. The results of trials on both materials indicated that changes in density diminish after compaction to energies of 450–700 kN m/m<sup>3</sup>. A standard compaction energy of 600 kN m/m<sup>3</sup> [ASTM D698 (ASTM 2000b)],

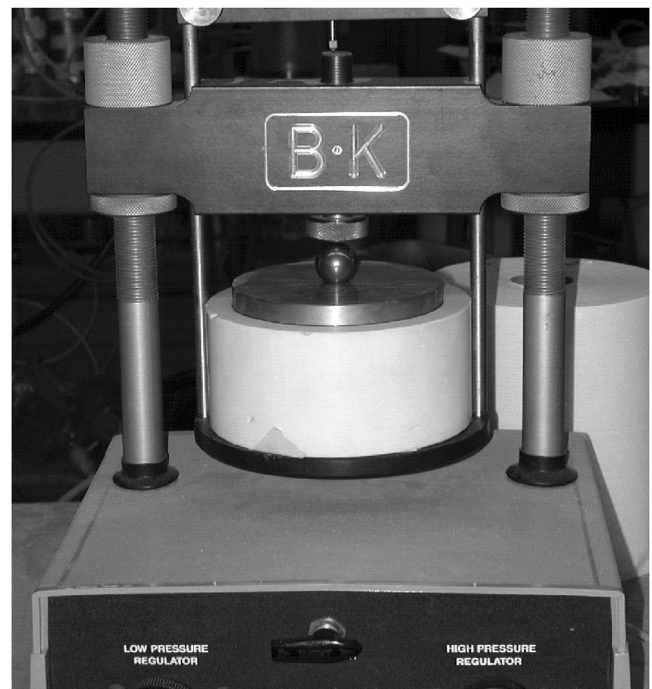


**Fig. 4.** Photograph of consolidation test device with oversized oedometer

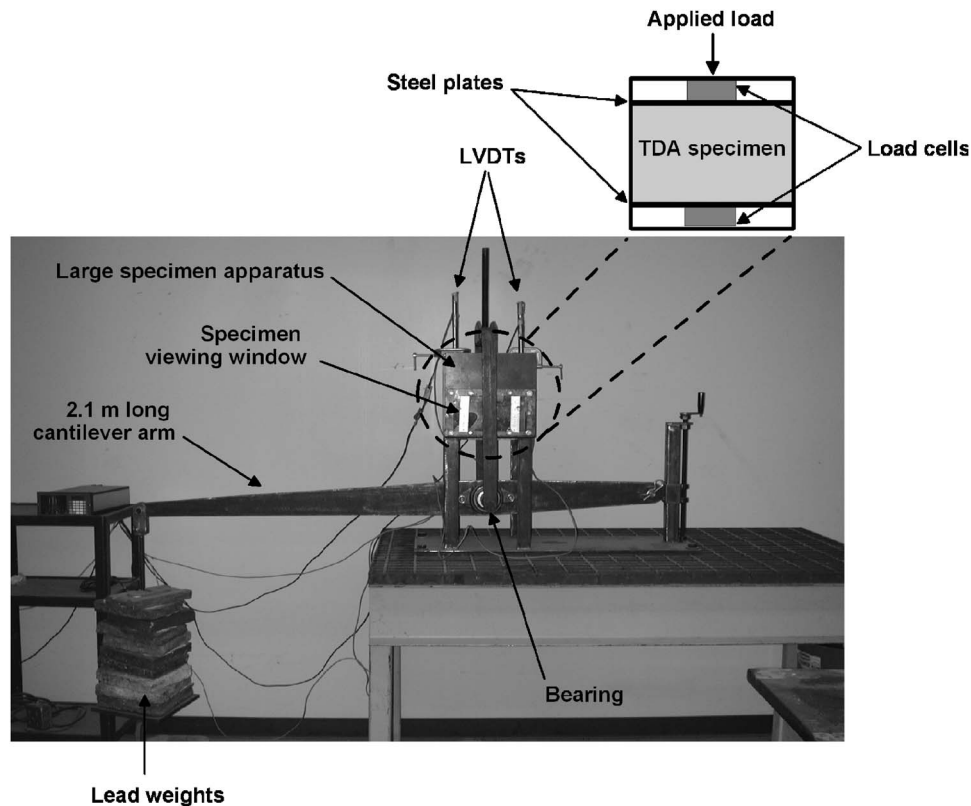


Fig. 5. Photograph of large cantilever test system showing details of the large specimen apparatus

which falls within this range, was adopted as the compaction criteria for these experiments. This resulted in relatively dense specimens when applied to the sand (0% TDA) and 50% TDA composite materials. Table 3 reports the compacted unit weights ( $\gamma$ ) for the tire chips and tire shreds based on this compaction criteria.

The relative magnitude of the as-compacted porosity ( $n$ ) values for TDA reported in Table 3 was supported by observations made during the specimen preparation. During mixing and compaction, the exposed metal reinforcing wire on the tire shreds frequently became entangled, making it difficult to effectively densify these materials through impact energy alone. This, in combination with the high aspect ratio of the tire pieces, resulted in relatively large as-compacted porosity values for the tire shreds. In contrast, the tire chips, with their low aspect ratio, minimal metal content, and broad gradation, have a comparatively lower porosity. This effect was apparent when looking at the particle matrix of the tire chips, which appeared to be dense and interlocked after compaction.

### Testing Procedures and Equipment

Two special compression test devices, an oversize oedometer and a large cantilever test system, were fabricated to accommodate the particle sizes of the tire chips and tire shreds. Both of these devices were housed in a temperature controlled laboratory. The oversize oedometer consisted of a floating Teflon ring mounted in a conventional pneumatic consolidation test device (Fig. 4). The oedometer had an inside dimension of 125 mm yielding a diameter to maximum particle size (tire chips) ratio of approximately 4:1. Also, the oedometer allowed for the testing of compacted specimens with an initial height of 73 mm, which is approxi-

mately three times greater than the maximum particle size of the tire chips. The sidewall of the oedometer was relatively thick (15 mm) to minimize lateral compliance. Trials performed with load cells placed directly above and below the specimen indicated that the combination of the Teflon ring and a light coating of nonsilicon grease on the inside wall yielded a low friction test system (sidewall friction  $<3\%$  of applied load). Applied stresses were monitored using a digital pneumatic pressure gauge whereas deformations were measured with a dial gauge. The size of the oedometer, while precluding the testing of tire shreds, made experimental setup and calibration easy, thus making the device well suited for performing both short and long duration parametric experiments on tire chips and tire chip-soil mixtures.

The second test device was a large cantilever test system (Fig. 5), which aside from its size, was otherwise similar to conventional gravity consolidation test frame. The gravity loading ensured that a constant stress was applied to the specimen over the duration of an experiment. The cantilever test system was used to test both tire chips and tire shreds. Specimens were tested in a 305 mm (inside dimension) square container with 13 mm thick steel sidewalls to minimize lateral compliance (this is hereafter referred to as the "large specimen apparatus"). One of the sidewalls included a 20 mm thick Plexiglas window, which allowed specimens to be directly observed during testing. The ratio of the inside dimension to maximum particle size ranged from 2.5:1 for the tire shreds to 12:1 for the tire chips. The square shape of the apparatus was better at accommodating placement of the rectangular tire shreds than a conventional circular device. The initial height of the specimens tested in the apparatus was typically about 200 mm. Prior to testing a light coating of nonsilicon grease was placed on the inside walls of the apparatus to mini-

mize sidewall friction. The inset diagram to Fig. 5 shows the large specimen apparatus in greater detail. Load cells were placed immediately below and above the specimen, thereby allowing sidewall friction to be directly measured. The sidewall friction, which was typically about 25% of the applied load, remained constant during the long-term tests. Sidewall friction was higher for the large specimen apparatus due to its square shape, which increased the perimeter contact area of the specimen, and because of the rougher steel sidewalls. Stress and deformation data were collected at regular intervals using an automated data acquisition system. When reducing the data, the stress in the specimen was assumed to be equal to the average of the stress values determined from the upper and lower load cells. For the immediate compression tests, the large specimen apparatus was placed in a conventional strain-controlled compression testing machine. Testing was performed at a constant strain rate of 7.5 mm/min. Owing to the large size of the equipment, experimental setup of the cantilever test frame was a time-consuming and laborious task and therefore only long duration experiments were performed with this device.

The experimental program also included several isotropic compression tests that were performed in a conventional automated triaxial test system. The size of the end platens limited the triaxial specimen diameter to approximately 75 mm, which precluded the testing of the tire shreds. The purpose of the triaxial tests was not to measure shear strength of TDA, but rather to determine how reductions in pore volume during compression contribute to overall volume change in the specimen. The tire chip specimens (100% TDA) were placed in latex membrane and compacted before being flushed with water and backpressure saturated. Once saturation “B-values” (Skempton 1954) of 0.97 or greater were achieved, the specimens were isotropically compressed and changes in specimen volume and void space were determined by measuring changes in the volume of water entering the cell (indicative of overall volume change in the specimen) and the volume of water expelled from the specimen (indicative of pore volume reduction) [Leong et al. 2004]. Changes in cell and specimen water volume were measured using instrumentation with a resolution of  $10^{-3}$  mL. The specimen volume changes presented in the following section include minor corrections ( $\approx 1.5\%$ ) to account for elastic deformation of the triaxial system (cell wall, connection rods, etc.). The correction factors were experimentally determined during separate trials by increasing the cell pressure while monitoring the cell water volume. Although small in magnitude, the correction factors were necessary to ensure accuracy in the measurements of the small volumes of water being measured.

## Compression Mechanisms

Isotropic compression tests were performed to identify the physical mechanism(s) that contribute to compression of TDA. Fig. 6 shows volume changes in TDA (100% tire chips) under saturated, drained, isotropic compression. Stresses were applied incrementally over a short time period to limit any appreciable time-dependent compression. The maximum applied stress was 550 kPa, which is at least an order of magnitude greater than the stresses encountered in typical geotechnical applications of TDA. Volume changes were normalized by the global volume of the specimen so that the results could be expressed in terms of the more relevant parameter of volumetric strain ( $\epsilon_{vol}$ ). Included in Fig. 6 are changes in water volume within the specimen, which is also expressed as volumetric strain (i.e., volume of water expelled

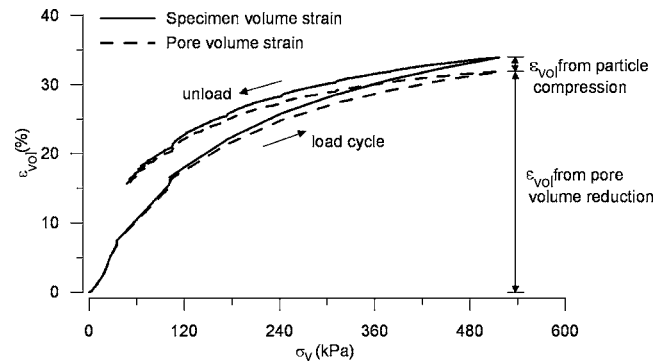


**Fig. 6.** Volume changes in TDA (tire chips) under saturated, drained, isotropic compression

from specimen divided by global specimen volume) to allow direct comparison with the specimen volumetric strains. Because the specimens were fully saturated, water expelled from the specimen during compression is directly attributable to pore volume reduction. Differences between the specimen and pore volume strains are a consequence of particle compression, whereas the pore volume strains alone result solely from the reduction of pore space.

The loading curve in Fig. 6 shows that the modulus ( $M$ ) (i.e., slope of the stress-strain curve) of TDA decreases with increasing applied stress, whereas the unload curve indicates that a significant fraction of the immediate compression is recoverable. At stresses up to approximately 120 kPa, the volume of water expelled from the specimen is nearly identical to the specimen volume change, implying that at these stress levels immediate compression is entirely a result of pore volume reduction. At larger stresses the difference between the specimen and pore volume response implies that the tire particles are compressing; however, volume change in the specimen is still largely dominated by reduction of pore volume. Therefore, it appears that particle compression does not contribute to immediate deformation of TDA at low to intermediate stresses. Even under high stresses (125 kPa and above) the contribution of particle compression to immediate deformation is, for practical purposes, negligible. It is worth noting that the gradation and appearance (based on visual inspection) of the tire particles was the same before and after the experiments, thereby indicating that particle damage (e.g., tearing, shearing, or crushing) did not play a role in pore volume reduction. This observation differs from that often made for sands, which usually experience some degree of particle crushing under similar levels of compressive stress (e.g., Cheng et al. 2004).

Fig. 7 shows specimen and pore volume response for a 100% tire chip specimen over the first 24 h of a continuous, isotropic stress at 80 kPa. The triaxial test data taken over longer time periods (i.e., several days or more) are thought to be less reliable due to the diminishing magnitude of the pore volume response and because of a variety of competing factors that affect the accuracy of the measurements such as creep/hysteresis of the test system and water absorption of the triaxial cell chamber and tire particles (Leong et al. 2004; Kuwano and Jardine 2002). The data shown in Fig. 7 indicate that the volume of the test specimen reduces with time, with the largest volume changes occurring during the first several hours of loading. Initially, there is a strong pore volume response that is close to the specimen volume change. This implies that, at least over initial time periods, time-dependent compression of TDA results primarily from pore

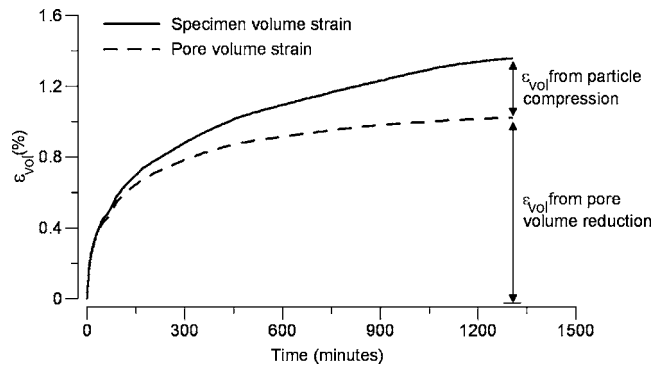


**Fig. 7.** Specimen and pore volume response for TDA specimen (tire chips) over the first 24 h of continuous, isotropic compression ( $\sigma_v = 80$  kPa)

volume reduction and secondarily from compression of the tire particles. With time the pore volume response slows even as the specimen continues to compress, indicating that particle compression becomes increasingly important as time progresses and eventually becomes the dominant mechanism of time-dependent compression.

### Immediate Compression

Experiments were performed to assess the effects of tire particle size and TDA content on the immediate deformation characteristics of TDA and TDA composites. Tests were performed under laterally restrained conditions in both the oversize oedometer and large specimen apparatus described earlier. Fig. 8 presents vertical strain as a function of applied stress for a series of tests performed on tire chips in the oedometer. For conditions of lateral confinement, vertical strains are equal to volumetric strains ( $\epsilon_v = \epsilon_{vol}$ ). Overall, for specimens with large TDA contents (85% and above), the first increments of stress result in significant compression after which the specimens become less compressible as strains accumulate and the material strain hardens. These results concur with data presented from other studies (Humphrey and Manion 1992; Ahmed 1993; Tatlisoz et al. 1997). The stress-strain curves for all specimens have the same general shape; however, in addition to obvious variation in magnitude, they differ in the amount of strain required to reach the onset of strain hardening. The curve shapes and data trends shown in Fig. 8 are typical of those for all short-

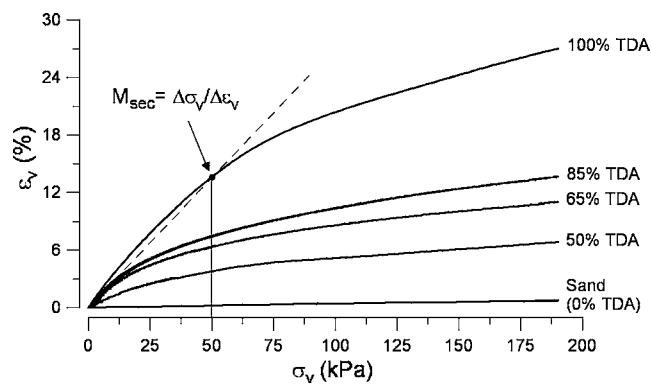


**Fig. 8.** Vertical strain ( $\epsilon_v$ ) versus stress ( $\sigma_v$ ) for TDA specimens (tire chips) tested in the oedometer

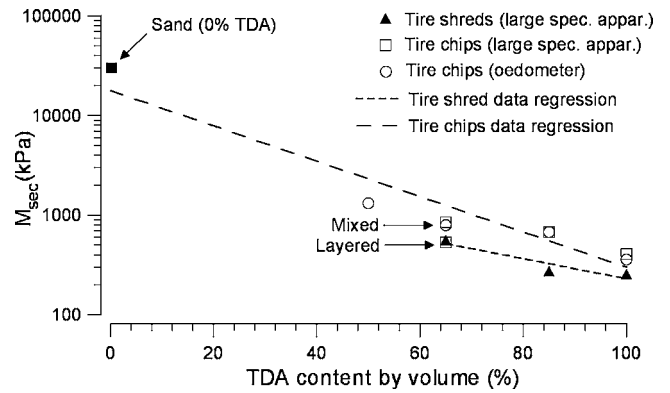


**Fig. 9.** Secant constrained modulus ( $M_{sec}$ ) versus TDA content for all specimens

term experiments, including the isotropic compression tests discussed earlier. In order to systematically evaluate the effect of TDA particle size and content, it was necessary to adopt a parameter to describe the stress-strain behavior. For this study the secant constrained modulus ( $M_{sec}$ ) was selected for this purpose and defined as (see Fig. 8)

$$M_{sec} = \frac{\Delta\sigma_v}{\Delta\epsilon_v} \quad (1)$$

Here,  $\Delta\sigma_v = 50$  kPa and  $\Delta\epsilon_v =$  change in vertical strain that occurs between 0 and 50 kPa. A vertical stress of 50 kPa was taken to be representative of typical overburden stress in TDA for a variety of common geotechnical applications. The secant constrained modulus ( $M_{sec}$ ) of TDA varied from a high of 1,320 kPa (50% tire chips) to a low of 255 kPa (100% tire shreds) with the most significant increase in constrained modulus (i.e., reduction in immediate compression) occurring with the addition of 15–35% sand.

The oedometer test on the 100% TDA specimen was repeated four times using tire chips from the same sample lot to assess the repeatability of the experimental results. These additional trials indicated that despite the seemingly heterogeneous nature of the tire chips, there was nevertheless an adequate degree of repeatability in the experimental results [ $M_{sec} (\bar{x} = 414$  kPa,  $\sigma = 42$  kPa)]. The consistency in the experimental results is likely due, in part, to the formal quality control procedures implemented at the TDA production facility to ensure uniformity in the product.

To more clearly illustrate the affects of TDA content on the compressibility of the mixtures, the oedometer test data (Fig. 8) are replotted as secant constrained modulus versus TDA content in Fig. 9. Also included in Fig. 9 are data from tests on tire chips and tire shreds performed in the large specimen apparatus. Several trends are apparent in Fig. 9.

- The TDA is approximately 20 times more compressible than the sand. The addition of just small amounts of sand (15–35%) reduces the immediate compressibility of the TDA by as much as 50%. Compressibility is further reduced, but at a decreasing rate (i.e., nonlinear), with the addition of larger quantities of sand. These observations pertain to both tire chip and tire shreds.
- The tire shreds and tire shred composites have constrained modulus values that are approximately 25% lower than those for comparable tire chip and tire chip composites. This is most likely related to the greater porosity of the tire shreds. This

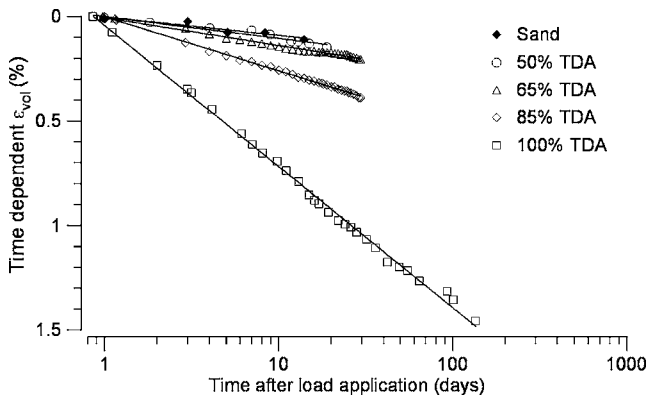


**Fig. 10.** Time-dependent volumetric strains ( $\epsilon_{vol}$ ) versus time for TDA (tire chips) tested in the oedometer ( $\sigma_v=80$  kPa). The data are shown with best fit logarithmic regression lines.

observation concurs with the statistical trend presented for constrained modulus and tire particle size by Strenk et al. (2007).

- There is virtually no difference between  $M_{sec}$  for the tire chips tested in the oedometer and the large specimen apparatus, suggesting that  $M_{sec}$  and the stress-strain response of the TDA were independent of the scale of the testing devices used in this study.
- The effects of TDA-soil interaction were considered by performing a test on a 65% tire chip mixture that was placed in two layers rather than being mixed before testing in the large specimen apparatus. The layered specimen yielded an  $M_{sec}$  value almost 50% lower than the comparable mixed specimen (Fig. 9). This suggests that at least for the 65% TDA specimen, interaction between the TDA and sand (probably through the filling of pore space) lowers the compressibility of TDA. Although based on limited data, this nevertheless highlights the

importance of ensuring that TDA composites are well mixed and that material segregation is minimized during field construction operations.

### Time-Dependent Compression

Time-dependent compression was investigated by performing experiments on specimens subjected to constant vertical stresses (35, 80, and 192 kPa) over time periods ranging from 3 to 28 weeks (average duration about 4 weeks). These experiments provided insight into the effect of tire particle size, TDA content, and the applied stress on the deformation characteristics of TDA and TDA composites over extended periods of time. Similar to the immediate compression experiments, tests were performed under laterally restrained conditions in both the oedometer and large specimen apparatus. Fig. 10 presents time-dependent volumetric strains in the specimens over several logarithmic cycles of time. The data in Fig. 10 is from tire chip specimens tested in the oedometer under a vertical stress of 80 kPa. Included in the figure are logarithmic regressions ( $R^2>0.95$ ) fit to data for times in excess of 1 day. This regression criterion was based on the observation that time-dependent compression reached a steady rate after 10 to 20 hours of testing and remained approximately constant over the remainder of the experiment. This indicates that representative time-dependent compression characteristics of TDA can be determined over the first several days of an experiment, and therefore extended duration tests ( $>5$  days) may not be needed in practice.

The data discussed above is plotted in Fig. 11 as the modified secondary compression index ( $C_{\alpha\epsilon}$ ) versus TDA content. Also included in Fig. 11 are data from tests performed on tire shreds as well as data for tire chips under different stresses. The modified secondary compression index is closely related to the secondary compression index ( $C_{\alpha}$ ), a parameter commonly used to quantify

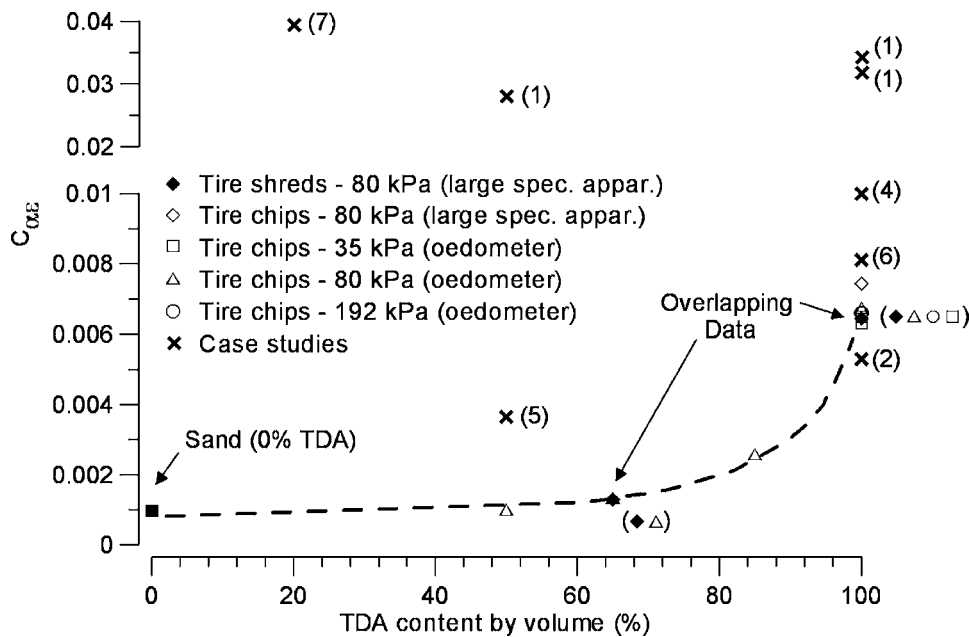


**Fig. 11.** Modified secondary compression index ( $C_{\alpha\epsilon}$ ) versus TDA content for laboratory test specimens and case studies. The number in parentheses refers to the case history data summarized in Table 1. The dashed line shows trends in the laboratory data (note the break in vertical scale).

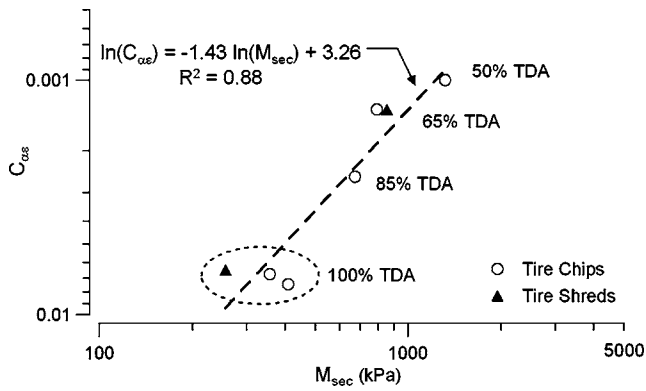


**Fig. 12.** Modified secondary compression index ( $C_{\alpha\epsilon}$ ) versus secant constrained modulus ( $M_{sec}$ ) for TDA composites. The dashed line shows the best-fit logarithm regression to the data.

secondary compression in fine-grained soil (Mesri 1973). This parameter was adopted for this work based on the accuracy with which it describes the experimental data and because of its routine use in engineering practice. For this study the parameter ( $C_{\alpha\epsilon}$ ) was defined as

$$C_{\alpha\epsilon} = \frac{\Delta \epsilon_{vol}}{\log \frac{t_2}{t_1}} \quad (2)$$

where  $\Delta \epsilon_{vol}$  = change in time-dependent volumetric strain,  $t_1$  = time when time-dependent compression begins, and  $t_2$  = time at which the magnitude of time-dependent compression is required.

The data shown in Fig. 11 indicate that tire chips exhibit a rate of time-dependent compression that is nearly an order of magnitude greater than sand. As was observed for immediate compression, there is a non-linear relationship between TDA content and time-dependent compression, with just small amounts of sand (15–25% by volume) yielding significant reductions in  $C_{\alpha\epsilon}$ . The modified secondary compression index ( $C_{\alpha\epsilon}$ ) of TDA varies from a high of 0.0074 (100% tire chips) to a low of 0.0010 (50% tire chips). For the tire shreds (100% TDA), time-dependent compression is shown to be only marginally lower than that of the tire chips. This differs from the scale dependence of  $M_{sec}$  observed for immediate compression. The  $C_{\alpha\epsilon}$  values for specimens with the same TDA content but different stresses are similar, implying that time-dependent compression is independent of applied stress. The repeatability of the time-dependent compression of TDA was assessed by performing three oedometer tests on tire chip specimens (100% TDA) from the same sample lot. As with immediate compression, these experiments indicated adequate repeatability [ $C_{\alpha\epsilon}$  ( $\bar{x}$  = 0.0054 and  $\sigma$  = 0.0009)]. Note that the  $C_{\alpha\epsilon}$  values summarized in Fig. 11 fall within the broad range of values presented for the field case study data summarized in Fig. 1.

For specimens tested under identical conditions, a relationship exists between immediate and time-dependent compression of the TDA and TDA composites (Fig. 12). This is similar in some respects to the established empirical relationship between coefficient of compression and secondary compression index in soil (Mesri and Godlewski 1977). In the absence of experimental results, the relationship shown in Fig. 12 could be used to provide a first estimate of  $C_{\alpha\epsilon}$  based on results of immediate compression tests.

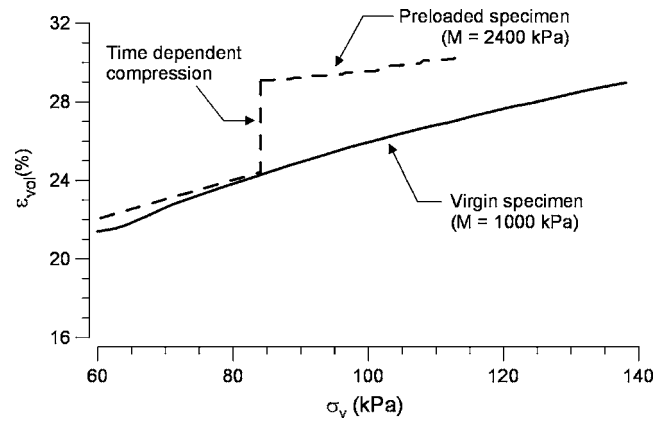


**Fig. 13.** Comparison of stress ( $\sigma_v$ ) versus volumetric strain ( $\epsilon_{vol}$ ) behavior for virgin (solid line) and preloaded (dashed line) TDA specimens

Fig. 13 compares experimental data over a selected stress range for specimens that have different stress histories, but are otherwise identical. The “virgin” specimen was subjected to a standard immediate compression experiment. The “preloaded” specimen was loaded to a stress of 80 kPa, which was then held for 4 weeks, after which the specimen was loaded to 110 kPa. The marked increase in modulus ( $M$ ) (i.e., slope of the stress-strain curve) for the preloaded specimen shows that the immediate compressibility of TDA reduces as time-dependent compression occurs.

## Discussion and Practical Implications

The high level of immediate compression in TDA is usually attributed to both its high porosity and compression of the individual tire particles. This study confirms the contribution of pore volume reduction to TDA compression, but demonstrates that particle compression is nonexistent or negligible, even at very large stresses. While the tire particles themselves do not compress, it is likely that their low elastic modulus contributes indirectly to the high compressibility of TDA by facilitating sliding, distortion, and rearrangement of pieces into denser, more stable arrangements under compressive load. Particle compression does appear to play a role, along with void reduction, in the time-dependent compression of TDA. The relative contribution of these two deformation mechanisms changes with time, with particle compression making a progressively greater contribution to compression as TDA ages.

Under short term loading, TDA is significantly more compressible than a typical granular soil; however, this may be of little practical significance for routine geotechnical engineering applications since these deformations would occur prior to completion of construction. Immediate compression resulting from transient loads, such as traffic, can usually be addressed through the design of a subbase soil layer of sufficient thickness [e.g., ASTM D6270 (ASTM 1998b)]. The densification associated with immediate compression will raise the unit weight of TDA by approximately 10% over laboratory-derived compacted values and this should be accounted for in design when computing consolidation of foundation soils underlying a TDA structure (Humphrey 2004c). This study has shown that the constrained modulus of TDA may increase by a factor of 100% or more as a conse-

quence of time-dependent compression. This has practical implications, for example, the design of pavement systems, which are usually designed based on immediate compression characteristics of virgin specimens (e.g., Humphrey and Manion 1992).

Time-dependent compression of TDA will occur over the service life of a typical geotechnical engineering project. Because immediate compression usually occurs prior to placement of settlement sensitive components, the deformations resulting from time-dependent compression may ultimately govern the long-term performance and serviceability of a TDA structure. The magnitude of time-dependent compression of TDA or TDA composites is a function of layer height, time, and TDA content. For this reason, time-dependent settlement will be most important when thick layers of TDA are used in geotechnical systems having long service lives. The experimental data indicate that time-dependent compression of TDA is independent of applied stress and tire particle size.

Although full-scale field experiments were not performed as part of this work, it is nevertheless useful to consider the laboratory test results in the context of the case history data presented earlier in Fig. 1 and Table 1. Logarithmic regressions ( $R^2=0.86-0.98$ ) were fit to the case history data to determine back-analyzed field values of  $C_{\alpha\epsilon}$ , which are included in Fig. 11 for comparison purposes. Data for postconstruction times of less than 10 days were excluded from the regression to ensure that the derived  $C_{\alpha\epsilon}$  values were not influenced by immediate compressing of the TDA or TDA composites. As indicated by the broken  $C_{\alpha\epsilon}$  scale in Fig. 11, two of the case studies [Zornberg et al. (2004b) and Bosscher et al. (1993)] yielded time-dependent compression values that greatly exceed those from the current laboratory study. However, two notable factors distinguish these test embankments from others available in the case study database: (1) The limited thickness of the TDA layer ( $<1.5$  m), and (2) the extreme nature of the surface load, which was largely comprised of truck traffic. Hence, time-dependent compression in these embankments may have been exacerbated by the heavy transient surface loads, which probably did not significantly attenuate within the thin layer of TDA or TDA composite. The other case study data presented in Fig. 11 (i.e., Tweedie et al. 1998; Humphrey et al. 2000; Dickson et al. 2001; Salgado et al. 2003; Hoppe and Mullen 2004) largely corroborates with the magnitude and trends in the laboratory data, suggesting that the results of this experimental study can be reliably extrapolated to large prototype TDA structures.

In practice, time-dependent compression is sometimes addressed by allowing 8 weeks to elapse after TDA placement before constructing settlement-sensitive components such as pavements (e.g., Tweedie et al. 2004). Applying the  $C_{\alpha\epsilon}$  values determined in this study ( $C_{\alpha\epsilon} \approx 0.0065$  for 100% tire shreds) to a typical TDA embankment suggests that this practice may be satisfactory for many applications. Time-dependent settlement ( $\Delta H_t$ ) is computed as

$$\Delta H_t = HC_{\alpha\epsilon} \log \frac{t_2}{t_1} \quad (3)$$

where  $H$ =thickness of the TDA layer;  $t_1$ =time when time-dependent compression begins (assumed to be 1 day); and  $t_2$ =time at which the magnitude of time-dependent compression is required.

For a typical embankment containing 3 m of TDA [Class II Fill, ASTM D6270 (1998b)], Eq. (3) yields time-dependent settlement of 3.5 cm after 2 months. An additional 1.5 and 2.9 cm of

displacement will occur after 1 and 5 years, respectively. Deformations of this magnitude are likely to be tolerable for many geotechnical systems. Not included in this computation is the additional settlement resulting from consolidation or secondary compression of the foundation soils underlying the embankment.

It is recommended that practitioners consider time-dependent settlement when designing TDA structures and determine the acceptability of these deformations on a case-by-case basis. This would allow construction delay times, if needed to mitigate time-dependent compression, to be determined on a project-specific basis. Although it is best to estimate  $C_{\alpha\epsilon}$  using project-specific materials and specimen preparation techniques, this may be cost prohibitive for routine projects due to the special laboratory equipment needed to accommodate the large tire particles. In these cases a first estimate of time-dependent settlement can be computed using the  $C_{\alpha\epsilon}$  values from this study.

The addition of soil will reduce both immediate and time-dependent compression of TDA, most likely because soil fills the pore volume in the TDA. Small to moderate amounts of soil (15–35%) can yield significant reductions in compressibility. To fully realize the benefits of soil augmentation, it is critical to ensure that the materials are thoroughly mixed and do not become segregated during placement and compaction. The task of preventing material segregation, although seemingly quite simple, was challenging even in the controlled laboratory environment. Ensuring this level of quality control for full-scale field operations may be a costly undertaking for constructors. Moreover, soil augmentation raises the unit weight, thereby affecting one of the most favorable characteristics of TDA.

## Conclusions

It has been shown that TDA exhibits high degrees of both immediate and time-dependent compression. The magnitude of immediate compression in TDA and TDA composites is principally a function of tire particle size, TDA content, and applied stress, whereas time-dependent compression is largely a function of TDA content and time. Immediate compression of TDA, which results almost entirely from the reduction of pore volume, increases with TDA content and tire particle size. A characteristic relationship between strain and time exists for TDA and TDA composites under one-dimensional confined compression. Both applied stress and tire particle size appear to have an insignificant effect on time-dependent compression in TDA.

With proper consideration of time-dependent settlement, TDA and TDA composites are appropriate for use in projects whose long-term performance and serviceability are affected by deformation. For cases where time-dependent settlement is judged to be excessive, one or more approaches may be employed to minimize its effects. These include (1) specifying a minimum time period between TDA placement and construction of settlement sensitive components, (2) preloading or surcharging the TDA layer over a specified time period, (3) soil augmentation, (4) reduction of TDA layer height, (5) tapering of the TDA layer from full height to zero over some distance, and (6) installation of structural appurtenances to help mitigate possible differential settlement at points of transition or interface with the TDA layer. Finally, it is worth noting that there are relatively little long-term field performance data for TDA structures and, as such, there remains an important need to monitor these structures over extended time frames to provide further validation for the findings of this study.

## Acknowledgments

Financial support for this research was provided in part by the National Science Foundation under Grant No. CMS-0134370. Any opinions, findings, and conclusions or recommendations expressed in this material are those of the writers and do not necessarily reflect the views of the National Science Foundation. Additional financial support for the third writer was provided in part by the Koerner Family Fellowship at Drexel University. Appreciation is expressed to Emmanuel Tires of Pennsylvania, who provided the TDA used in this study. The thoughtful comments provided by anonymous reviewers improved this paper.

## Notation

The following symbols are used in this paper:

- $C_\alpha$  = secondary compression index;  
 $C_{\alpha s}$  = modified secondary compression index;  
 $D_{\max}$  = maximum particle size (or average maximum particle dimension);  
 $e$  = void ratio;  
 $G_s$  = specific gravity;  
 $H$  = thickness of TDA layer;  
 $H_t$  = time-dependent settlement;  
 $M$  = slope of the stress ( $\sigma_v$ )-strain ( $\epsilon_{\text{vol}}$ ) curve;  
 $M_{\text{sec}}$  = secant constrained modulus at  $\sigma_v=50$  kPa;  
 $n$  = porosity;  
 $R^2$  = coefficient of determination;  
 $t_i$  = time;  
 $\bar{x}$  = mean;  
 $\gamma$  = compacted unit weight (TDA) or maximum dry density (sand);  
 $\epsilon_v$  = vertical strain;  
 $\epsilon_{\text{vol}}$  = volumetric strain;  
 $\sigma$  = standard deviation; and  
 $\sigma_v$  = vertical stress.

## References

- Ahmed, I. (1993). "Laboratory study on properties of rubber soils." *Rep. No. FHWA/IN/JHRP-93/4*, Dept. of Civil Engineering, Purdue Univ., West Lafayette, Ind.
- ASTM. (1998a). "Classification of soils for engineering purposes." *D2487-93*, West Conshohocken, Pa.
- ASTM. (1998b). "Standard practice for use of scrap tires in civil engineering applications." *D6270-98*, West Conshohocken, Pa.
- ASTM. (2000a). "Test method for laboratory compaction characteristics of soil using modified effort." *D1557-00*, West Conshohocken, Pa.
- ASTM. (2000b). "Test method for laboratory compaction characteristics of soil using standard effort." *D698-00*, West Conshohocken, Pa.
- ASTM. (2005). "Test method for density, relative density (specific gravity), and absorption of coarse aggregate." *C127-04*, West Conshohocken, Pa.
- Bosscher, P. J., Edil, T. B., and Eldin, N. (1993). "Construction and performance of shredded waste tire embankment." *Transportation Research Record. 1345*, National Research Council, Transportation Research Board, Washington, D.C., 44–52.
- Bosscher, P. J., Edil, T. B., and Kuraoka, S. (1997). "Design of highway embankments using tire chips." *J. Geotech. Geoenviron. Eng.*, 123(4), 295–304.
- Cheng, Y. P., Bolton, M. D., and Nakata, Y. (2004). "Crushing and plastic deformation of soils simulated using DEM." *Geotechnique*, 54(2), 131–141.
- Cosgrove, T. A. (1995). "Interface strength between tire shreds and geomembrane for use as a drainage layer in a landfill cover." *Proc., Geosynthetics '95*, Industrial Fabrics Association, St. Paul, Minn., Vol. 3, 1157–1168.
- Dickson, T. H., Dwyer, D. F., and Humphrey, D. N. (2001). "Prototype tire-shred embankment construction." *Transportation Research Record. 1755*, National Research Council, Transportation Research Board, Washington, D.C., 160–167.
- Edil, T. B. (2002). "Mechanical properties and mass behavior of shredded tire-soil mixtures." *Proc., Int. Workshop on Light-Weight Geomaterials*, Tokyo, 17–32.
- Edil, T. B., and Bosscher, P. J. (1994). "Engineering properties of tire shreds and soil mixtures." *Geotech. Test. J.*, 17(4), 453–464.
- Foose, G. J., Benson, C. H., and Bosscher, P. J. (1996). "Sand reinforced with shredded waste tires." *J. Geotech. Engrg.*, 122(9), 760–767.
- Hoppe, E. J., and Mullen, W. G. (2004). "Field study of a shredded-tire embankment in Virginia." *Rep. No. VTRC 04-R20*, Virginia Transportation Research Council, Charlottesville, Va.
- Humphrey, D. N. (2004a). "Tire derived aggregate—A new geomaterial for your toolbox." *Geo-Strata—Geo Institute of ASCE*, 5(2), 20–22.
- Humphrey, D. N. (2004b). "Effectiveness of design guidelines for use of tire derived aggregate as lightweight embankment fill." *Recycled materials in geotechnics*, A. H. Aydilek and J. Wartman, eds., Geotechnical Special Publication No. 127, ASCE, Baltimore, 61–74.
- Humphrey, D. N. (2004c). "Civil engineering applications of tire shreds." *California integrated waste management board*, California Environmental Protection Agency, Sacramento, Calif.
- Humphrey, D. N., and Manion, W. P. (1992). "Properties of tire chips for light-weight fill." *Proc., Grouting, Soil Improvement, and Geosynthetics*, Vol. 2, ASCE, New York, 1344–1355.
- Humphrey, D. N., Sandford, T. C., Cribbs, M. M., Gharegrat, H. G., and Manion, W. P. (1992). "Tire chips as light-weight backfill for retaining walls—Phase I." *A study for the New England Transportation Consortium*, Dept. of Civil Engineering, Univ. of Maine, Orono, Me.
- Humphrey, D. N., Sandford, T. C., Cribbs, M. M., and Manion, W. P. (1993). "Shear strength and compressibility of tire chips for use as retaining wall backfill." *Transportation Research Record. 1422*, National Research Council, Transportation Research Board, Washington D.C., 29–35.
- Humphrey, D. N., Whetten, N., Weaver, J., and Recker, K. (2000). "Tire shreds as lightweight fill for construction on weak marine clay." *Proc., Int. Symp. on Coastal Geotechnical Engineering in Practice*, Balkema, Rotterdam, The Netherlands, 611–616.
- Kuwano, R., and Jardine R. J. (2002). "On measuring creep behaviour in granular materials through triaxial testing." *Can. Geotech. J.*, 39(5), 1061–1074.
- Leong, E. C., Agus, S. S., and Rahardjo, H. (2004). "Volume change measurement of soil specimen in triaxial test." *Geotech. Test. J.*, 27(1), 1–10.
- Mesri, G. (1973). "Coefficient of secondary compression." *J. Soil Mech. and Found. Div.*, 99(1), 123–137.
- Mesri, G., and Godlewski, P. M. (1977). "Time- and stress-compressibility interrelationship." *J. Geotech. Engrg. Div.*, 103(5), 417–430.
- Moo-Young, H., Sellasie, K., Zeroka, D., and Sabnis, G. (2003). "Physical and chemical properties of recycled tire shreds for use in construction." *J. Environ. Eng.*, 129(10), 921–929.
- Salgado, R., Yoon, S., and Siddiki, N. Z. (2003). "Construction of tire shred test embankment." *Rep. No. FHWA/IN/JTRP-2002/35*, Indiana Dept. of Transportation, Indianapolis.
- Skempton, A. W. (1954). "The pore pressure coefficients A and B." *Geotechnique*, 4(4), 143–147.
- Strenk, P. M., Wartman, J., Grubb, D. G., Humphrey, D. N., and Natale, M. F. (2007). "Variability and scale-dependency of tire derived aggregate." *J. Mater. Civ. Eng.*, 19(3).
- Tatlısoz, N., Benson, C. H., and Edil, T. B. (1997). "Effect of fines on

- mechanical properties of soil-tire chip mixtures.” *Testing soil mixed with waste or recycled materials, STP 1275*, M. Wasemiller, and K. Hoddinott, eds., ASTM, West Conshohocken, Pa., 93–108.
- Tweedie, J. J., Humphrey, D. N., and Sandford, T. C. (1998). “Tire chips as light-weight backfill for retaining walls—Phase II.” *A study for the New England Transportation Consortium*, Dept. of Civil Engineering, Univ. of Maine, Orono, Me.
- Tweedie, J. J., Humphrey, D. N., and Wight, M. H. (2004). “Old town-mud pond inlet bridge, rehabilitation of a timber structure with tire shreds.” *Proc., Geotrans*, ASCE, Reston, Va., 740–749.
- Wu, W. Y., Benda, C. C., and Cauley, R. F. (1997). “Triaxial determination of shear strength of tire chips.” *J. Geotech. Geoenviron. Eng.*, 123(5), 479–482.
- Yang, S., Lohnes, R. A., and Kjartanson, B. H. (2002). “Mechanical properties of shredded tires.” *Geotech. Test. J.*, 25(1), 44–52.
- Youwai, S., and Bergado, D. T. (2003). “Strength and deformation characteristics of shredded rubber tire-sand mixtures.” *Can. Geotech. J.*, 40(1), 254–264.
- Zornberg, J. G., Cabral, A. R., and Chardphoom, V. (2004a). “Behavior of tire shred-sand mixtures.” *Can. Geotech. J.*, 41(1), 227–241.
- Zornberg, J. G., Costa, Y. D., and Vollenweider, B. (2004b). “Performance of prototype embankment built with tire shreds and nongranular soil.” *Transportation Research Record. 1874*, National Research Council, Transportation Research Board, Washington, D.C., 70–77.